

Utah State University

DigitalCommons@USU

---

Undergraduate Honors Capstone Projects

Honors Program

---

5-2003

## Predicting Mountain Pine Beetle Development with the Extended von Foerster Model

Jeffrey Tullis Leek  
*Utah State University*

Follow this and additional works at: <https://digitalcommons.usu.edu/honors>



Part of the [Mathematics Commons](#)

---

### Recommended Citation

Leek, Jeffrey Tullis, "Predicting Mountain Pine Beetle Development with the Extended von Foerster Model" (2003). *Undergraduate Honors Capstone Projects*. 834.

<https://digitalcommons.usu.edu/honors/834>

This Thesis is brought to you for free and open access by the Honors Program at DigitalCommons@USU. It has been accepted for inclusion in Undergraduate Honors Capstone Projects by an authorized administrator of DigitalCommons@USU. For more information, please contact [digitalcommons@usu.edu](mailto:digitalcommons@usu.edu).



PREDICTING MOUNTAIN PINE BEETLE  
DEVELOPMENT WITH THE EXTENDED  
VON-FOERSTER MODEL

by

Jeffrey Tullis Leek

Thesis submitted in partial fulfillment  
of the requirements

for

UNIVERSITY HONORS WITH DEPARTMENTAL HONORS

in

Mathematics

Approved:

---

James Powell  
(Thesis Advisor)

---

James Powell  
(Departmental Honors Liaison)

---

Tom Peterson  
(Director of the Honors Program)

UTAH STATE UNIVERSITY  
Logan, UT  
2003

# Predicting Mountain Pine Beetle Development with the Extended von Foerster Model

Jeffrey Leek  
Department of Mathematics and Statistics  
Utah State University  
Logan, UT 84322-3900,  
U.S.A.

April 25, 2003

## Abstract

The mountain pine beetle (*Dendroctonus ponderosae* Hopkins) represents a significant threat to ponderosa pine and lodgepole pine stands in the western United States, and has the potential to threaten commercially valuable jack pine in both the United States and Canada. The success of the mountain pine beetle is based on synchronization of developmental events to time cold-hardened life stages for extreme winter temperatures and to facilitate mass attack and overwhelm the defenses of the host. This paper presents a solution methodology for an extended McKendrick - von Foerster model for the development of the mountain pine beetle in varying temperature environments. The model reflects the effect of phenotypic variability on output, and is suitable for determining field distributions of emergence events. An efficient computational method, based on Green's functions, is presented. Results are compared with direct numerical simulation, and the modelling and simulation strategy is applied to determine the distribution of emergence for mountain pine beetles. Eventually these results will be applied to improve forest management strategies in regard to the epidemic outbreak of pine beetles in northwestern North America.

# Contents

<b>1</b>	<b>Introduction</b>	<b>5</b>
<b>2</b>	<b>The Extended von Foerster Model</b>	<b>6</b>
<b>3</b>	<b>Applying the Extended von Foerster Model</b>	<b>10</b>
3.1	Convolution Solution Method . . . . .	10
3.2	Direct Solution Method . . . . .	14
3.3	Analytic Solution . . . . .	20
<b>4</b>	<b>Results</b>	<b>20</b>
4.1	Comparison of Solution Techniques . . . . .	20
4.2	Comparison of Empirical Data and Convolution Solution . . . . .	21
<b>5</b>	<b>Conclusion</b>	<b>26</b>
<b>6</b>	<b>Appendix A</b>	<b>29</b>
<b>7</b>	<b>Appendix B</b>	<b>30</b>

## List of Figures

1	The accumulated variance of the population $\nu$ versus developmental rate $r$ for all life stages and temperatures. The figure casts doubt on the assumption of the Sharpe et al. model that there exists a linear relationship between $\nu$ and $r$ [3]. . . . .	7
2	Population distribution estimated by the distributed delay model for individuals at age $a = 1$ , where $(\lambda, \Delta a) = (15, 0.02)$ , $(7.5, 0.02)$ , and $(5, 0.03)$ . Although each distribution has the same mean, the standard deviation is clearly dependent on $\Delta a$ , the arbitrary width of each phase [3]. . . . .	8
3	The developmental rate functions for the mountain pine beetle across the eight life stages used in the extended von Foerster model. In physical situations temperature also varies with time [7]. . . . .	11
4	A flowchart outlining the MATLAB program used to compute the results of equation (3). The user inputs an initial population $\vec{p}_0$ and an initial temperature $\vec{T}$ , the necessary computations are made for one life stage, and the output population $\vec{p}_1$ becomes the input for the next life stage. This loop is repeated for each of the 8 life stages. . . . .	12
5	A method for efficient evaluation of the denominator in the convolution code. A time matrix is created with the time steps running down columns, along with its transpose. When the two are subtracted the rows can be packed one by one, taking advantage of symmetry to speed calculations. . . . .	15
6	A method for efficient evaluation of the rates integral in the convolution code. First a cumulative rates integral is established with the cumulative rates appearing across columns. The difference between the cumulative rates matrix and its transpose gives the rates integral in the exponent of the convolution (3). The convolution can then be packed into a series of vectors taking advantage of symmetry for efficient calculation. . . . .	16
7	A flowchart outlining the MATLAB program used to compute the results of equation (9). The user inputs an initial population $\vec{p}_0$ and an initial temperature $\vec{T}$ , the necessary computations are made for one life stage, and the output population $\vec{p}_1$ becomes the input for the next life stage. This loop is repeated over all age and time steps. . . . .	18
8	The results for the first life stage from the numerical, convolution, and analytic solutions to the extended von Foerster model. The initial population for all programs is (16) evaluated at $a = 1$ and the boundary condition is $p(0, a) = 0$ . The discretization for the numeric solution is $(\Delta t, \Delta a) = (.04, .04)$ . The population distributions from the three programs are almost identical, demonstrating that the two numerical approximations accurately represent the analytic solution for constant $\nu$ and $r$ . . . . .	22
9	The results of the Convolution and Numeric Programs for $(\Delta t, \Delta a) = (0.2, 0.1)$ , $(0.04, 0.04)$ , and $(0.001, 0.005)$ respectively for the 7th life stage. The figure demonstrates that as $\Delta a$ and $\Delta t$ go to zero the direct numeric solution converges to the convolution solution. In the final graph the two produce nearly identical plots. . . . .	23

10 The results of the extended von-Foerster model using the empirical population density from 2001 and the temperature series from probed trees plotted against data collected in the summer of 2002 in the SNRA. . . . . 25

# 1 Introduction

The Mountain Pine Beetle (*Dendroctonus ponderosae* Hopkins) represents a significant threat to ponderosa pine (*Pinus ponderosae* Lawson) and lodgepole pine (*Pinus contorta* Douglas) stands in the western United States, and has the potential to threaten commercially valuable jack pine (*Pinus banksiana* Lambert) [6]. Adult beetles attack a tree and deposit their eggs in the phloem. The larvae hatch and eat the phloem, interrupting circulation and effectively girdling the tree, which is generally fatal to the host. In addition beetles act as a delivery vector for the pathogenic blue stain fungus, which kills pines and lowers their commercial value. As a method of defense pines flood beetle egg galleries with resin. To overcome this defense, the Mountain Pine Beetle (MPB) must attack synchronously in great numbers to overwhelm the tree.

Synchronization of attacks is essential to the survival and reproduction of MPB, as is an appropriate seasonality. To be successful, adult beetles must time their cold-hardened life stages for winter and their emergence for August, when the trees are under the greatest stress. Complicating matters further, MPB pass through 8 life stages, each with a distinct rate of development, and all dependent on temperature [15]. It has also been shown that, while there is no evidence of diapause in the MPB, seasonal temperature can synchronize life cycles and facilitate mass attack [5, 8, 9, 10, 14]. Because of its commercial and ecological significance, models which predict the phenology and seasonality of MPB are quite important.

Two of the models currently used to predict the development of poikilothermic organisms have been implemented in variable temperature environments. The probabilistic Sharpe et al. model is based on assumptions about control enzymes and can be used to find the predicted distribution of emergence dates, or emergence distribution, of mountain pine beetles [5, 11, 12, 3]. This model depends on the assumption that the mean and standard deviation of the developmental rate are proportional to determine how variance accumulates as populations develop. The plot of accumulated variance versus developmental rate in Figure (1) seems to contradict this assumption, as no linear relationship is apparent between the mean and

standard deviation. An alternative approach, distributed delay models, divide the life stages of an organism into discrete "phases" [3, 13]. Populations flow from one phase to the next at given rates, and as a consequence the developmental rate ( $r$ ) and the accumulation of variance, depend on the length of the phases. If  $\Delta a$  represents the length of a phase and  $\lambda\Delta a$  is the mean developmental rate, then figure (2) demonstrates that the choice of  $\Delta a$  for this model can not be arbitrary if  $\lambda\Delta a$  is held constant. Each choice of  $\Delta a$  produces a different distribution. While there has been some success in developing models that take the choice of  $\Delta a$  into account, these models are still only appropriate for a range of phase size values [8].

A third approach, the von Foerster model, was originally developed to model cell division, and has been extended to many other applications. An extension described in this paper introduces a term to account for accumulating variance over life stages. Here we develop two numerical solution techniques for the extended von Foerster equation. The first is a solution based on convolution techniques. The second employs a direct numerical approximation of the equation. Both schemes are implemented over all 8 stages of the mountain pine beetle life cycle using empirically determined functions for the rates of development and accumulation of variance within each stage. The two solution methods are shown to be consistent and the predictive power of the model is tested against data collected in the Sawtooth National Recreation Area.

## 2 The Extended von Foerster Model

The von-Foerster equation is given by:

$$\frac{\partial}{\partial t}p(a, t) + \frac{\partial}{\partial a}p(a, t) = g(a, t, p(a, t)).$$

where  $t$  is laboratory time,  $a$  is age (or the fraction of life stage completed),  $T(t)$  is temperature as a function of time,  $p(a, t)$  is the population density of individuals at age  $a$  and time  $t$ , and  $g(a, t, p(a, t))$  is the total increase or decrease in the size of the population [3]. Although



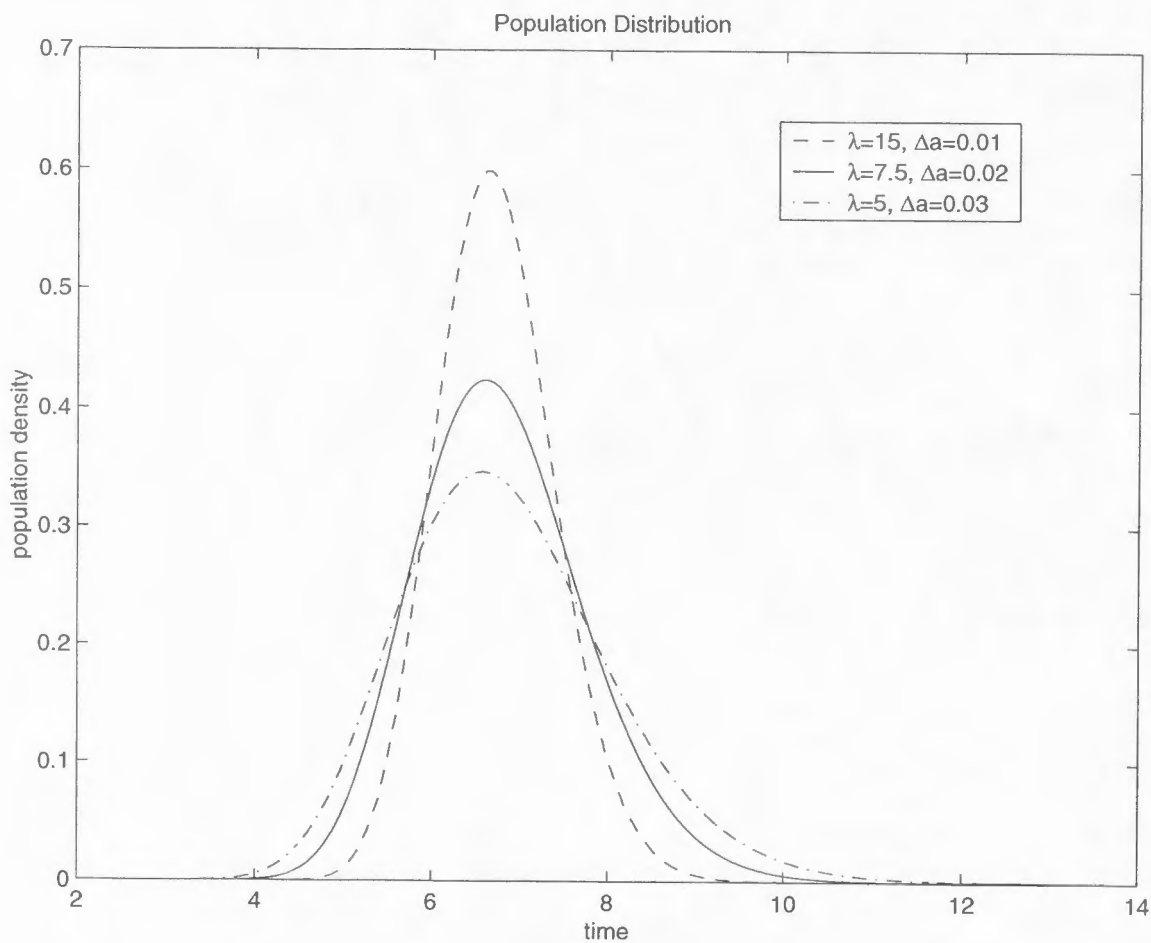


Figure 2: Population distribution estimated by the distributed delay model for individuals at age  $a = 1$ , where  $(\lambda, \Delta a) = (15, 0.02)$ ,  $(7.5, 0.02)$ , and  $(5, 0.03)$ . Although each distribution has the same mean, the standard deviation is clearly dependent on  $\Delta a$ , the arbitrary width of each phase [3].

the von-Foerster equation was originally created to model cell division, it has been extended to apply to many different processes, including: natural forest age dynamics, population resensitization in cycling cells exposed to ionizing radiation, and analysis of intraspecific competition between adults and juveniles [4, 1, 2]. A variation of this equation used to model MPB development is given by:

$$\frac{\partial}{\partial t}p(a, t) + r(T(t))\frac{\partial}{\partial a}p(a, t) = \nu(T(t))\frac{\partial^2}{\partial a^2}p(a, t) \quad (1)$$

where  $r(T(t))$  and  $\nu(T(t))$  are the developmental and variability rates for each life stage as a function of temperature (which may vary with time). The developmental rate is the inverse of the time to emergence for the mountain pine beetle, and the variability rate is related to the accumulated variance across life stages for the population. The model was developed by Gilber (2002) based on an analysis of the flux of individuals through small age intervals. The model assumes an underlying population of beetles with developmental rates sampled from a normal distribution with mean  $r$  and standard deviation  $\sigma$ , where  $\sigma$  is the standard deviation in developmental rate for the beetle population [3]. The parameter  $\nu = \frac{\sigma^2}{2}$  controls the accumulation of variance across the population over time and is assumed to be constant over each life stage as the parameter varies only slightly with temperature within each life stage. The equation describing the  $j^{th}$  life stage is given by:

$$\begin{aligned} \frac{\partial p_j}{\partial t} + r_j(T(t))\frac{\partial p_j}{\partial a} &= \nu_j \frac{\partial^2 p_j}{\partial a^2}, \quad 0 < t, \quad 0 < a \leq 1, \\ p_1(a, 0) &= 0, \quad 0 < a \leq 1, \\ p_1(0, t) &= p_{j-1}(a = 1, t), \quad 0 < t, \end{aligned} \quad (2)$$

where  $p_{j-1}$  is the population distribution of the  $(j-1)^{st}$  life stage and  $r_j(T(t))$  and  $\nu_j$  are the developmental rate and variability in the  $j^{th}$  stage. The number of beetles passing into the  $j^{th}$  life stage is determined by the number leaving the  $(j-1)^{st}$  life stage, thus the boundary condition is the population of the  $(j-1)^{st}$  stage evaluated at  $a = 1$ , or when the beetles reach the boundary of the stage. This equation is then iterated over the life cycle of the

MPB, using the respective  $r$  and  $\nu$  for each stage and the output from the previous stage ( $\vec{p}_{j-1}(1, t)$ ) as the input for determining the following stage ( $\vec{p}_j(0, t)$ ). The rate functions were determined empirically and in general are nonlinear. Figure (3) depicts the rates as a function of temperature (see Appendix B for complete rate functions and parameter descriptions), although in a physical situation temperature also varies as a function of time. The output from the final iteration is the predicted population distribution for the next generation.

### 3 Applying the Extended von Foerster Model

#### 3.1 Convolution Solution Method

The solution to Equation (2) derived with Green's functions is (see Appendix A for a complete derivation of this solution):

$$p_j(1, t) = \int_0^t f(\tau) \frac{H(t - \tau)}{\sqrt{4\pi\nu_j(t - \tau)^3}} \exp \left[ \frac{-(1 - \int_\tau^t r_j(T(s)) ds)^2}{4\nu_j(t - \tau)} \right] d\tau \quad (3)$$

A numerical MATLAB program was coded to evaluate the solution defined in (3). The flowchart in Figure (4) outlines the steps involved in the implementation of the convolution code.

The process is outlined in detail in *PSEUDOCODE* (1):

#### PSEUDOCODE (1)

**Step 1** *The hourly input temperature vector  $\vec{T}$  is converted into a matrix that is  $24 \times (\text{nyears} \cdot 365)$ , where nyears is the number of years of data. After this conversion the temperature series over each day is represented by a column of the matrix, making integrating over days the sum over columns.*

**Step 2** *A separate loop selects the appropriate variability constant,  $\nu_j$ , and rates function,  $r_j(\vec{T}(j), \vec{P})$ , for each life stage. The rates are computed as a function of temperature ( $\vec{T}(n)$ ) and input parameters ( $\vec{P}$ ) specific to the mountain pine beetle (see Appendix B).*

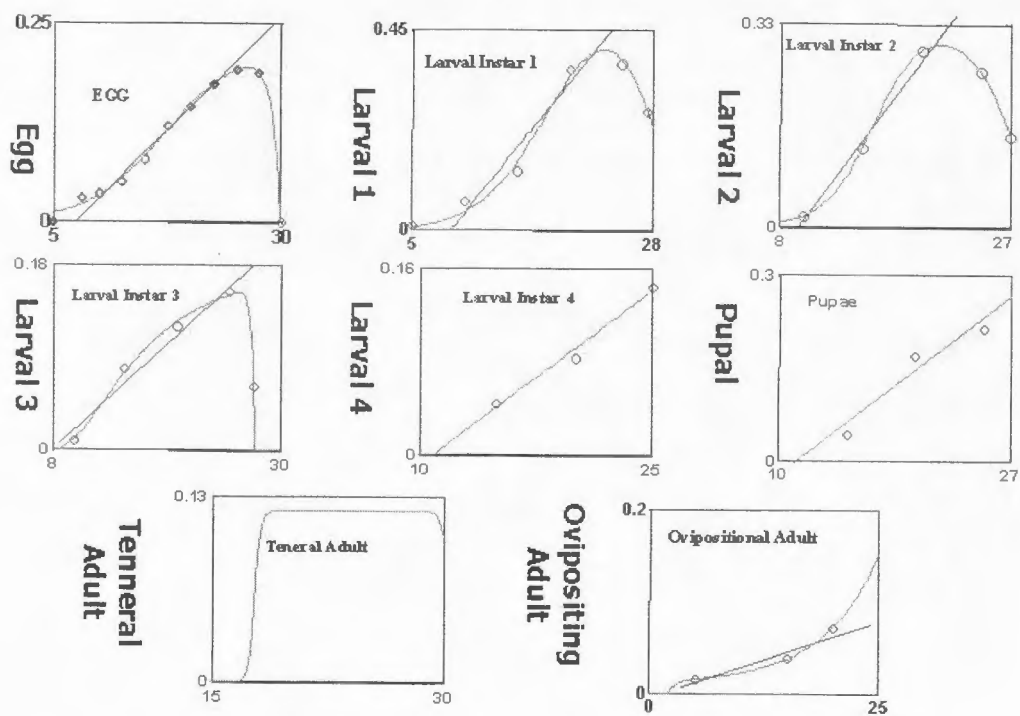


Figure 3: The developmental rate functions for the mountain pine beetle across the eight life stages used in the extended von Foerster model. In physical situations temperature also varies with time [7].

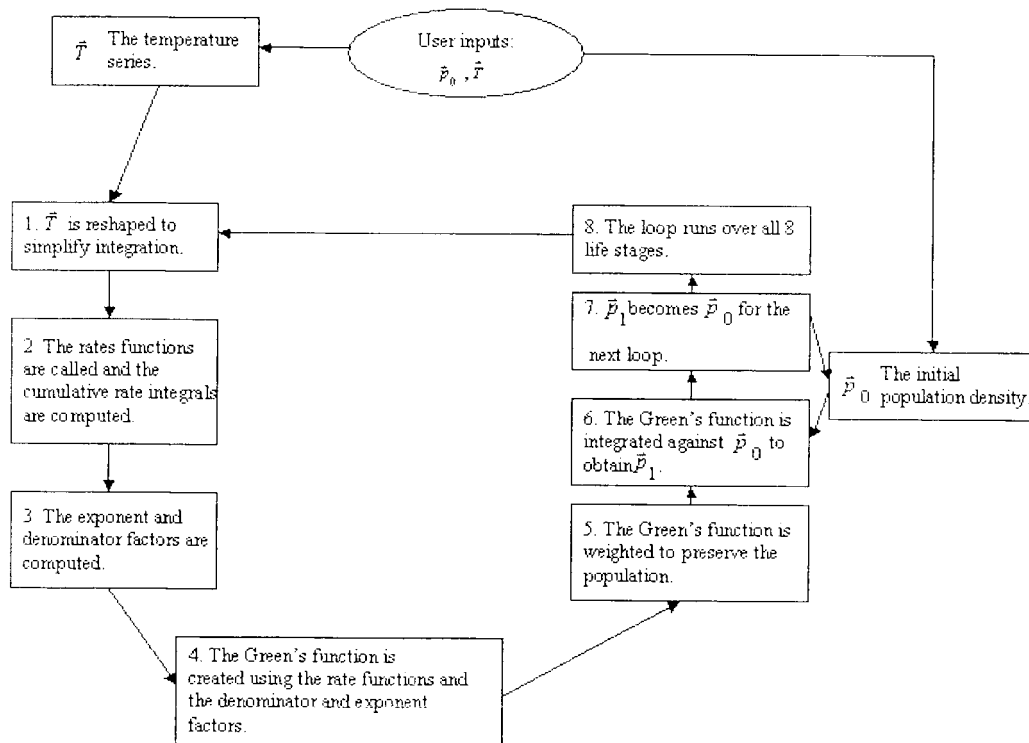


Figure 4: A flowchart outlining the MATLAB program used to compute the results of equation (3). The user inputs an initial population  $\vec{p}_0$  and an initial temperature  $\vec{T}$ , the necessary computations are made for one life stage, and the output population  $\vec{p}_1$  becomes the input for the next life stage. This loop is repeated for each of the 8 life stages.

**Step 3** The exponent  $\vec{E}$  and denominator  $\vec{D}$  factors are computed term by term over all time values:  $\vec{E}(n) = \frac{1}{(4\nu\vec{t}(n))}$  and  $\vec{D}(j) = \frac{1}{\sqrt{4\nu\pi\vec{t}(n)}}$ , where  $\vec{t}(n)$  is the  $n^{\text{th}}$  value of the time vector.

**Step 4 (i).** The cumulative rates vector  $\vec{C}(n) = \sum_{k=1}^n \vec{r}_j(\vec{T}(k))$  and one minus the cumulative value of the rates vector are stored:  $\vec{C}_1(n) = 1 - \sum_{k=1}^n \vec{r}_j(\vec{T}(k))$ .

**(ii).** A series of time vectors are created that store the values of the time vector from  $n+1$  to  $t_f - n + 1$  where  $t_f$  is the final time value.

**(iii).** The exponent and denominator factors are evaluated at these time vectors to yield the convolution in the denominator and exponent of equation (3).

**(iv).**  $\vec{C}_1$  is evaluated from  $n+1$  to  $t_f - 1$ , and the  $n^{\text{th}}$  value of  $\vec{C}$  is added to it to create a series of cumulative rates vectors for the integral in the convolution exponent of equation (3).

**(v).** The denominator, exponent, and rates function factors, along with the time vectors are combined to create the Green's function:  $\vec{GF} = \exp[-\vec{E} \cdot (\vec{C}_1 + \vec{C})^2 \cdot \vec{D}]$

**Step 5** The Green's function ( $\vec{GF}$ ) is normalized by dividing by the sum of its values to preserve the overall population from life stage to life stage. If the sum is smaller than a certain tolerance, skip this step.

**Step 6** The output is the result of multiplying term by term the Green's function by the input  $\vec{p}_0$ :  $\vec{p}_1(n) = \vec{p}_0(n) \cdot \vec{GF}(n)$

**Step 7** The output vector  $\vec{p}_1$  is saved and replaces  $\vec{p}_0$  and the loop begins again with Step 4.

The loop in Pseudocode (1) is repeated 8 times using a different rate function and variability constant for each life stage. **Step 4(ii)** creates a series of time vectors for efficient computation of the denominator factor in the convolution (3). The process is outlined in

Figure (5). **Step 4**(*iii*) and (*iv*) “pack” the matrix of cumulative rate values into a series of vectors that can be evaluated more rapidly (see Figure (6)). The process takes advantage of symmetry in the cumulative rate matrix to make the computation more efficient. The program produces a normalized population density function for each life stage of MPB. The final output is the predicted emergence distribution for the mountain pine beetles. The “packing” process results in an approximately 80% reduction in computation time.

### 3.2 Direct Solution Method

To corroborate the results obtained from the optimized convolution solution method a discrete numerical approximation was created. The first step in the numerical calculation was to discretize the age-time domain without compromising the stability of the solution (see the von-Neumann analysis below). Next a flux form of the partial differential equation was derived. The flux form was derived to conserve the number of individuals across life stages and to resolve the discontinuities in the rate functions along the boundary of the stages. After this change (1) becomes:

$$\frac{\partial}{\partial t}p(a, t) = -\frac{\partial}{\partial a} \left( r(T(t))p(a, t) - \nu \frac{\partial}{\partial a}p(a, t) \right). \quad (4)$$

The flux is defined as:

$$F = r(T(t))p(a, t) - \nu \frac{\partial}{\partial a}p(a, t).$$

A hybrid of the central difference and upwinding schemes are then applied. At the  $a = 0$  boundary the condition:

$$p_{j,0}^n = f(n\Delta t),$$

holds, where  $f$  is the population distribution over time of eggs at  $a = 0$ ,  $\Delta a$  and  $\Delta t$  are the age and time steps, and  $p_{j,i}^n$  is the population evaluated at time  $n\Delta t$ , age  $i\Delta a$  and life stage  $j$ . At the  $a = 1$  boundary of the final age step a radiative boundary condition is applied to allow beetles to pass through the boundary without affecting the rest of the domain. The

## Matrix Evaluation of the Denominators

$$T = \begin{pmatrix} 1 & 2 & 3 & \dots & t_f \\ 1 & 2 & & \dots & t_f \\ 1 & & \ddots & & \vdots \\ \vdots & \dots & & \ddots & \vdots \\ 1 & 2 & \dots & \dots & t_f \end{pmatrix}$$

- Create two square matrices, T and Y.
- Matrix T has the values of t in each of its columns.
- Matrix Y has the values of t in each of its rows.

$$Y = \begin{pmatrix} 1 & 1 & 1 & \dots & 1 \\ 2 & 2 & & \dots & 2 \\ 3 & & \ddots & & \vdots \\ \vdots & \dots & & \ddots & \vdots \\ t_f & t_f & \dots & \dots & t_f \end{pmatrix}$$

## Matrix Evaluation of the Denominators (cont.)

$$|T-Y| = \begin{pmatrix} 0 & 1 & 2 & \dots & t_f-1 \\ 1 & 0 & 1 & \dots & t_f-2 \\ 2 & 1 & 0 & \dots & t_f-3 \\ \vdots & \vdots & & \ddots & \vdots \\ t_f-1 & t_f-2 & \dots & \dots & 0 \end{pmatrix}$$

- Subtract the two matrices (T-Y).
- Take the absolute value.
- The values of (t-y) appear on the rows.

## Efficient Evaluation of the Denominator

$$\vec{t} = [1 \quad 2 \quad 3 \quad \dots \quad t_f]$$

- Create a vector with the values of t.

$$\vec{t}_i = [i+1 \quad i+2 \quad \dots \quad t_f-i+1]$$

- Create a series of vectors containing the values of t from i+1 to t\_f-i+1.

Figure 5: A method for efficient evaluation of the denominator in the convolution code. A time matrix is created with the time steps running down columns, along with its transpose. When the two are subtracted the rows can be packed one by one, taking advantage of symmetry to speed calculations.

### Matrix Evaluation of the Rates Integral

$$R = \begin{pmatrix} \int_0^0 r(s) ds & \int_0^1 r(s) ds & \int_0^2 r(s) ds & \dots & \int_0^v r(s) ds \\ \int_0^0 r(s) ds & \int_0^1 r(s) ds & \dots & \dots & \int_0^v r(s) ds \\ \vdots & \vdots & \ddots & \ddots & \vdots \\ \int_0^0 r(s) ds & \dots & \dots & \dots & \int_0^v r(s) ds \end{pmatrix}$$

- Create the rates matrix R.
- Each row of R contains the cumulative integral of r.

### Matrix Evaluation of the Rates Integral (cont.)

$$R_c = \begin{pmatrix} \int_0^0 r(s) ds & \int_0^1 r(s) ds & \int_0^2 r(s) ds & \dots & \int_0^v r(s) ds \\ \int_0^1 r(s) ds & \int_0^1 r(s) ds & \dots & \dots & \int_0^v r(s) ds \\ \vdots & \vdots & \ddots & \ddots & \vdots \\ \int_0^v r(s) ds & \dots & \dots & \dots & \int_0^v r(s) ds \end{pmatrix}$$

- Create the matrix  $R_c = R - R^T$ .
- $R_c$  contains the convolved rates integrals in its rows.

### Efficient Rates Integral

$$R_c = \begin{pmatrix} \int_0^0 r(s) ds & \int_0^1 r(s) ds & \int_0^2 r(s) ds & \dots & \int_0^v r(s) ds \\ \int_0^1 r(s) ds & \int_0^1 r(s) ds & \dots & \dots & \int_0^v r(s) ds \\ \vdots & \vdots & \dots & \dots & \vdots \\ \int_0^v r(s) ds & \dots & \dots & \dots & \int_0^v r(s) ds \end{pmatrix}$$

- Create the matrix  $R_c = R - R^T$ .
- We only need to the values of  $R_c$  above the diagonal.
- So pack upper triangular portion of  $R_c$  along the rows.

### Efficient Rates Integral (cont.)

$$\begin{bmatrix} \int_0^1 r(s) ds & \int_0^2 r(s) ds & \int_0^3 r(s) ds & \dots & \int_0^v r(s) ds \\ \int_0^2 r(s) ds & \int_0^3 r(s) ds & \int_0^4 r(s) ds & \dots & \int_0^v r(s) ds \\ \vdots & \vdots & \vdots & \ddots & \vdots \\ \int_0^v r(s) ds & \int_0^v r(s) ds & \int_0^v r(s) ds & \dots & \int_0^v r(s) ds \end{bmatrix}$$

- Create a vector with the cumulative integral of rates.
- Create a series of vectors that contain the elements of  $r$  from  $i+1$  to  $t_f$ .
- Subtract the value of the  $i^{\text{th}}$  element of  $r$ .

Figure 6: A method for efficient evaluation of the rates integral in the convolution code. First a cumulative rates integral is established with the cumulative rates appearing across columns. The difference between the cumulative rates matrix and its transpose gives the rates integral in the exponent of the convolution (3). The convolution can then be packed into a series of vectors taking advantage of symmetry for efficient calculation.

population density after one time step is approximated by:

$$p_{j,i}^{n+1} = p_{j,i}^n + \frac{\Delta t}{\Delta a} \left( F_{j,i-\frac{1}{2}}^n - F_{j,i+\frac{1}{2}}^n \right) + O(\Delta t^2) \quad (5)$$

with:

$$F_{j,i-\frac{1}{2}}^n = r_- p_{j,i}^n - \nu_- \frac{p_{j,i}^n - p_{j,i-1}^n}{\Delta a} \quad (6)$$

$$F_{j,i+\frac{1}{2}}^n = r_+ p_{j,i+1}^n - \nu_+ \frac{p_{j,i+1}^n - p_{j,i}^n}{\Delta a} \quad (7)$$

substituting the expressions for the flux terms (6),(7) into (5) produces (8).

$$p_{j,i}^{n+1} = p_{j,i}^n + \frac{\Delta t}{\Delta a} \left[ r_- p_{j,i}^n - r_+ p_{j,i+1}^n - \nu_- \frac{p_{j,i}^n - p_{j,i-1}^n}{\Delta a} + \nu_+ \frac{p_{j,i+1}^n - p_{j,i}^n}{\Delta a} \right] \quad (8)$$

Where the values  $r_-$  and  $\nu_-$  are the values of the rate function and variability constant on the left side of the node, and  $r_+$  and  $\nu_+$  are the values on the right side. Along the boundaries for life stages (when  $a = 1$  in the solution), there are discontinuities in the rate function and variability constant. To model these jumps the plus and minus rate function and variability constant must be used. Equation (8) can also be written as:

$$p_{j,i}^{n+1} = (c1)p_{j,i-1}^n + (c2)p_{j,i}^n + (c3)p_{j,i+1}^n \quad (9)$$

where:

$$c1 = r_- \frac{\Delta t}{\Delta a} + \nu_- \frac{\Delta t}{\Delta a^2} \quad (10)$$

$$c2 = 1 - \left[ r_+ \frac{\Delta t}{\Delta a} + \frac{\nu_+ \Delta t}{\Delta a^2} + \frac{\nu_- \Delta t}{\Delta a^2} \right] \quad (11)$$

$$c3 = \frac{\nu_+ \Delta t}{\Delta a^2} \quad (12)$$

to maintain simplicity in the code. The results from this numerical technique were computed using MATLAB. The process is outlined in the flowchart in Figure (7).

A more explicit description of the implementation appears in Pseudocode (2):

### PSEUDOCODE (2)

**Step 1** The input population  $\vec{p}_0 = (p_0^1, p_0^2, \dots, p_0^{t_f})$  where  $t_f$  is the final time step, is integrated over all time values to produce the weighting constant for each output population.

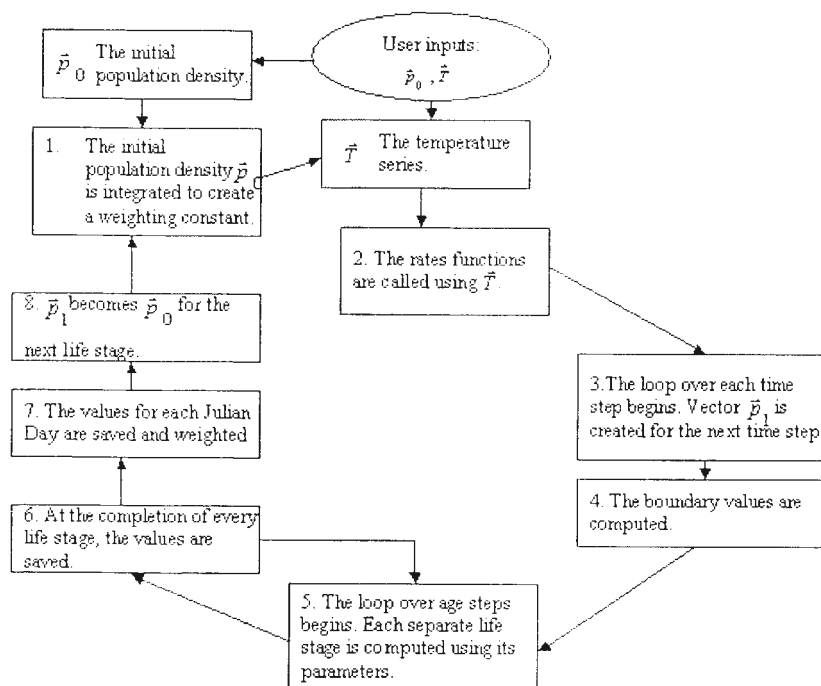


Figure 7: A flowchart outlining the MATLAB program used to compute the results of equation (9). The user inputs an initial population  $\vec{p}_0$  and an initial temperature  $\vec{T}$ , the necessary computations are made for one life stage, and the output population  $\vec{p}_1$  becomes the input for the next life stage. This loop is repeated over all age and time steps.

- Step 2** *The rates are computed as a function of temperature ( $\vec{T}(j)$ ) and input parameters ( $\vec{P}$ ) specific to the mountain pine beetle (see Appendix B).*
- Step 3** *Vector  $\vec{p}_1$  is defined as the value at the next time step.*
- Step 4** *The values of  $p_0^1$  and  $p_1^1$  are computed using the boundary conditions from equation (2).*
- Step 5** *The loop over life stages begins. The age vector is divided into 8 equal intervals. Away from the boundaries  $r_- = r_+$  and  $\nu_- = \nu_+$  in equations (10), (11), and (12). At the boundaries the rates functions and variability constants differ. Equation (9) is evaluated at every age step.*
- Step 6** *At the end of each loop the population distribution at a specific life stage (egg, larvae, etc.) is saved, then steps 5 and 6 are repeated over each life stage.*
- Step 7** *After all eight life stages have been completed, the values of  $p_1$  are saved at particular time intervals (i.e. each Julian Day).*
- Step 8**  *$\vec{p}_1 = (p_1^1, p_1^2, \dots, p_1^f)$  is set to  $\vec{p}_0$ , the old  $\vec{p}_1$  is cleared, and the loop begins again at Step 3.*

The results of a standard von Neumann analysis show that the scheme is stable provided that the conditions  $\frac{\nu \Delta t}{\Delta a^2} \leq \frac{1}{2}$  and  $\max_{T(t)} \left( \frac{r(T(t)) \Delta t}{\Delta a} < 1 \right)$  hold. The first requirement means  $\Delta t$  may be many orders of magnitude smaller than  $\Delta a$ . For example, if  $\Delta a = .001$ , we have  $\Delta t = .00001$ , and for decreasing values of  $\Delta a$  the difference becomes greater. Thus for a discretization smaller than  $\Delta a = .01$  the program can take hours to complete. Even more costly are the varying rate functions  $r_j$  and variability constants  $\nu_j$  for the eight life stages that make it necessary to create a nested loop structure to evaluate the approximation over all age and time values. The convolution code bypasses these difficulties and can produce the same results much more rapidly.

### 3.3 Analytic Solution

To verify the accuracy of the two solution methods an analytic solution can be derived. It is assumed that the rate and variance parameters take on constant values for each life stage. Applying the Laplace transform to (1) produces a second order linear differential equation,

$$s\hat{p} - p(a, 0) = -r\hat{p}_a + \nu\hat{p}_{aa}, \quad (13)$$

$$p(a, 0) = 0,$$

$$p(0, s) = 1.$$

The solution to (13) is:

$$p(a, s) = c_1 \exp\left[\frac{1}{2} \frac{r + \sqrt{r^2 + 4\nu s}}{\nu}\right] + c_2 \exp\left[\frac{1}{2} \frac{r - \sqrt{r^2 + 4\nu s}}{\nu}\right]. \quad (14)$$

Since the solution must be bounded, set  $c_1 = 0$ . Furthermore, from the boundary condition,  $c_2 = 1$ . After application of these two conditions the solution to the differential equation is,

$$p(a, s) = \exp\left[\frac{1}{2} \frac{r - \sqrt{r^2 + 4\nu s}}{\nu}\right]. \quad (15)$$

The analytic solution (16) is the inverse laplace transform of (15).

$$p(a, t) = \frac{a}{\sqrt{4\pi\nu t^3}} \exp\left[-\frac{(1 - rt)^2}{4\nu t}\right]. \quad (16)$$

The solution determined in equation (16) can be coded into a numeric MATLAB program and compared with the other solution techniques to test their accuracy for constant values of the rate functions  $r_j$  and and variability constants  $\nu_j$ . Note that the analytic solution matches the convolution solution (3) when a constant value of  $r_j$  is assumed.

## 4 Results

### 4.1 Comparison of Solution Techniques

Each of the three programs (analytic, convolution based, and direct approximation) was run with  $r = .05$  and  $\nu = .007$  constant. The initial condition for all programs was equation (16)

evaluated at  $a = 1$  and the boundary condition was  $p(0, a) = 0$ . The temperature series for each was a constant  $T = 12^\circ \text{ C}$ . The discretization for the numeric solution was  $(\Delta t, \Delta a) = (.04, .04)$ . The plots obtained from the analytic, convolution, and numeric MATLAB programs with  $r = .05$  and  $\nu = .007$  for the first life stage are shown in Figure (8).

The graph clearly shows that for constant  $r$  and  $\nu$  the analytic, convolution, and numeric techniques produce nearly the same population distributions. The correlation coefficient is  $r^2 \approx 0.9938$  for the analytic and numeric solutions and  $r^2 \approx 1.0000$  for the analytic and convolution solutions. The approximation is assumed to be accurate to  $O(\Delta t, \Delta a)$ , and the values of the correlation coefficient are well within this order of accuracy.

Another comparison between the numeric and convolution techniques was performed using varying rate functions and variability constants. For this experiment, temperature was sinusoidal with an amplitude of  $2^\circ \text{ C}$  and mean at  $17^\circ \text{ C}$ . The rate functions were those shown in Figure (3) and the variability was held constant across each life stage but varied between life stages. In order to demonstrate that the solutions match asymptotically the results for several values of  $\Delta t$  and  $\Delta a$  are shown in Figure (9). The plot shown is the output from the seventh life stage for both programs.

The correlation coefficients for  $(\Delta t, \Delta a) = (0.2, 0.1), (0.04, 0.04)$ , and  $(0.001, 0.002)$  are 0.8333, 0.9361, and 0.9934 respectively. From these values we can see that as the intervals approach zero, the direct numeric approximation seems to be converging to the convolution based solution. From Figure (9) it is clear that the solutions are converging graphically as well confirming our assumption that the convolution code provides an accurate numerical solution to equation (2).

## 4.2 Comparison of Empirical Data and Convolution Solution

The use of the extended von Foerster model as a tool for the prediction of emergence events is contingent on its accuracy in predicting the peaks in the population distribution for each life stage. To validate the model, data was collected in the Sawtooth National Recreation

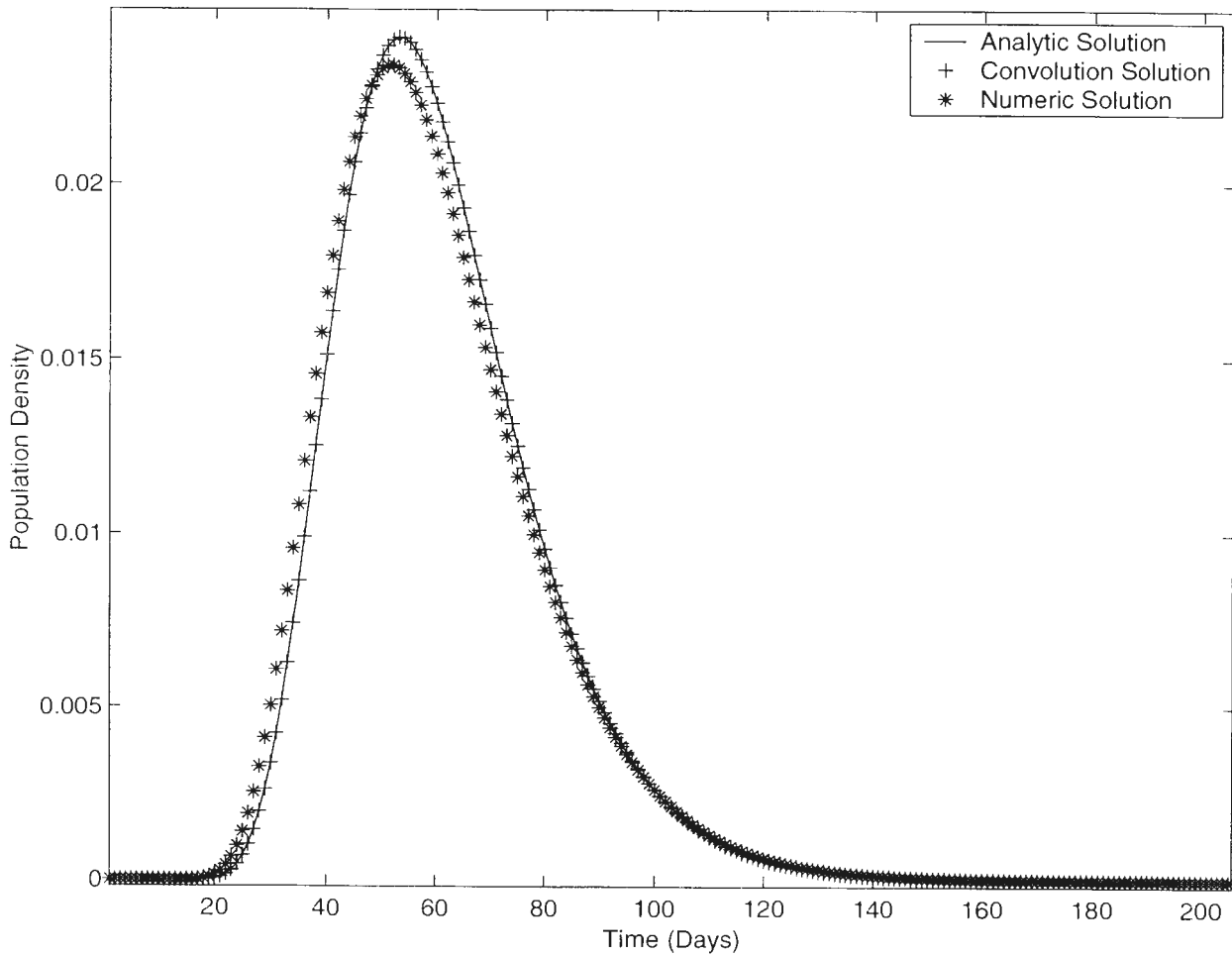


Figure 8: The results for the first life stage from the numerical, convolution, and analytic solutions to the extended von Foerster model. The initial population for all programs is (16) evaluated at  $a = 1$  and the boundary condition is  $p(0, a) = 0$ . The discretization for the numeric solution is  $(\Delta t, \Delta a) = (.04, .04)$ . The population distributions from the three programs are almost identical, demonstrating that the two numerical approximations accurately represent the analytic solution for constant  $\nu$  and  $r$ .

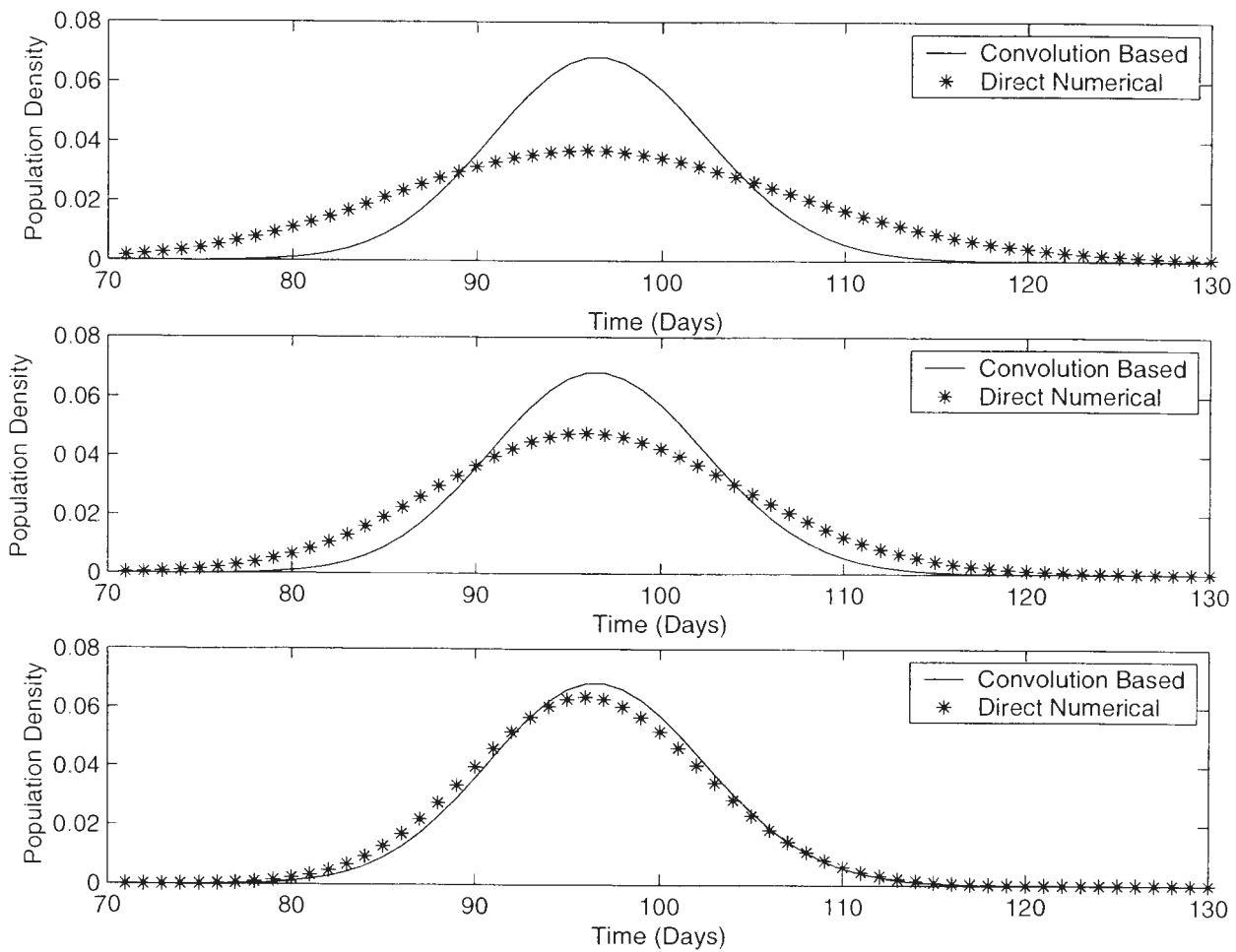


Figure 9: The results of the Convolution and Numeric Programs for  $(\Delta t, \Delta a) = (0.2, 0.1)$ ,  $(0.04, 0.04)$ , and  $(0.001, 0.005)$  respectively for the 7th life stage. The figure demonstrates that as  $\Delta a$  and  $\Delta t$  go to zero the direct numeric solution converges to the convolution solution. In the final graph the two produce nearly identical plots.

Area (SNRA).

Selected trees in the SNRA were marked in May 2001, and the number of MPB attacking each tree was observed on a daily basis. In addition to counting the attacks, each tree was mounted with a temperature probe that monitored the temperature of the tree in the developmental environment of the MPB under the bark. The following summer (2002), beetles from the marked trees were collected using mesh "traps" developed at the Rocky Mountain Research Station. The traps were collected on a daily basis and the number of beetles that emerged was noted. In Figure (10) the output of the production convolution code using the empirical population density from 2001 and the temperatures from the probes is plotted against the actual emergence data collected from the SNRA in the summer of 2002.

The "activity" term was added to model flight activity of the mountain pine beetle. Since the MPB is poikilothermic, its metabolism is directly related to temperature. The metabolism of the MPB is not fast enough to allow flight unless the temperature is above 18° C for approximately 5 hours. Incorporating this observation gives an "activity" correction to the last life stage.

From Figure (10) we can see that the von Foerster model, particularly with the activity term, is useful for describing general trends in the emergence behavior of the mountain pine beetle. The discrepancy between the observation and the predicted behavior may be attributed to a variety of factors. The small number of trees that were checked for emergence may not provide an accurate representation of the emergence behavior of the population as a whole. The empirical curve represents an average emergence over several trees at one location. Individual trees may experience slightly different environmental pressures, which may influence the accuracy of the prediction. Factors such as temperature differences due to snow pack, varying degrees of shade and sunlight, and many other small environmental fluctuations may contribute to the differences between the predicted result and the data.

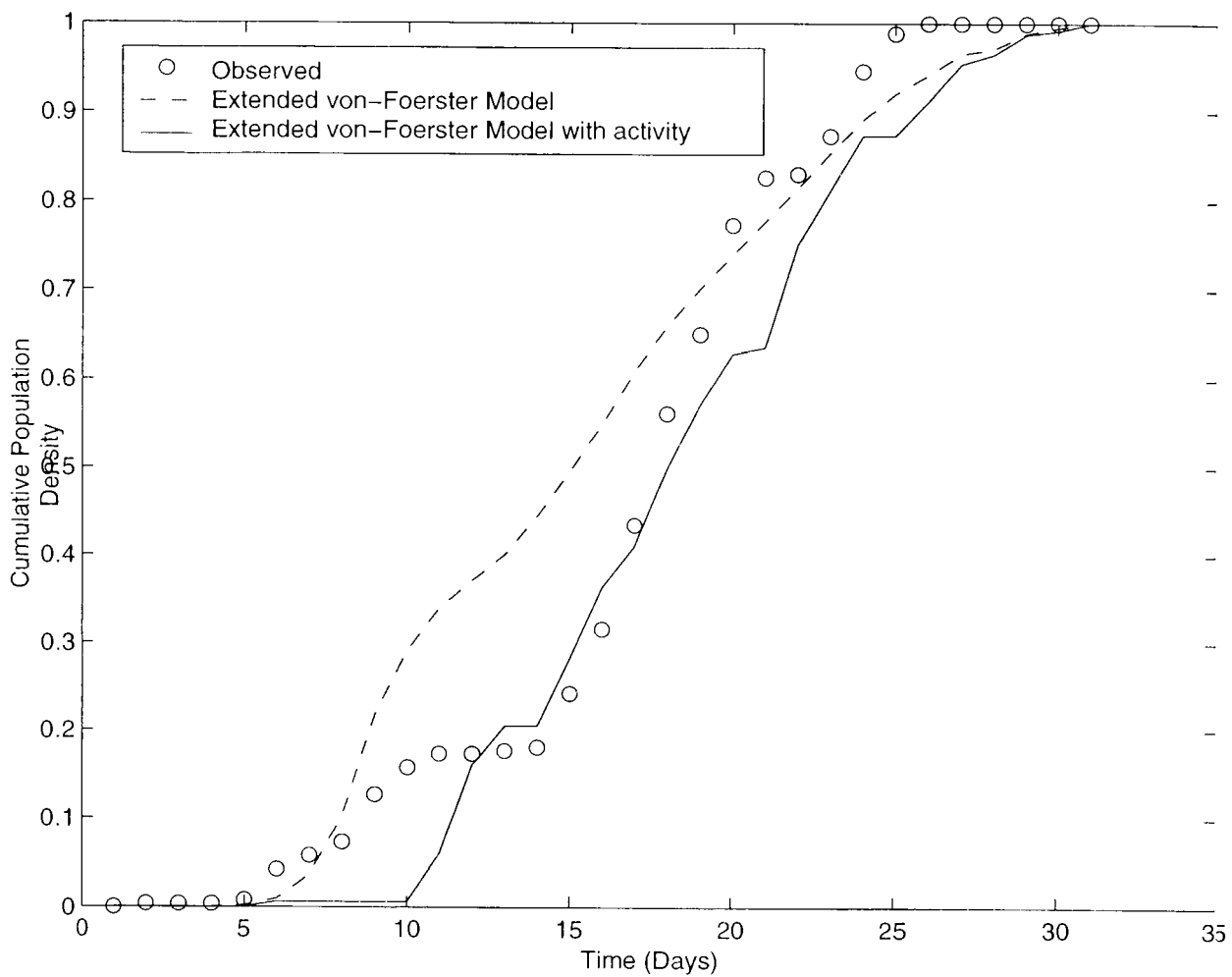


Figure 10: The results of the extended von-Foerster model using the empirical population density from 2001 and the temperature series from probed trees plotted against data collected in the summer of 2002 in the SNRA.

## 5 Conclusion

The convolution solution to the extended von Foerster model matches the analytic and numeric solutions for constant rate functions. Furthermore for rate functions that depend on temperature the numeric solution approaches the convolution solution asymptotically. Therefore the convolution solution is an accurate representation of the behavior of the model in varying temperature regimes. In addition, the convolution solution of the von Foerster model compares favorably with observations from field sites.

Modeling phenologic events is the first step toward a forest level predictive model of the mountain pine beetle outbreak in Northwestern North America. The next step is to evaluate potential combinations of temperature models with the convolution solution. Eventually the results will be incorporated into spatial models of mountain pine beetle attacks currently under development.

## References

- [1] Chen P.L., D.J. Brenner, and R.K. Sachs (1995). Ionizing radiation damage to cells: Effects of cell cycle redistribution. *Math. Biosciences* 126(2):147-170.
- [2] Cushing J.M. and J. Li (1991). Juvenile versus adult competition. *J. Math. Biology* 29(5):457-474.
- [3] Gilbert, E. (2002). Masters Thesis. Utah State University, Logan, Utah.
- [4] Kraemer, M.A., L.V. Kalachev, and D.W. Coble (2002). A class of models describing age structure dynamics in a natural forest. *Natural Resource Modeling* 15(2):149-200.
- [5] Logan, J.A. and G.D. Amman (1986). A distribution model for egg development in mountain pine beetle. *Can. Entomol.* 118:361-372.
- [6] Logan, J.A. and B.J. Bentz (1999). Model analysis of mountain pine beetle seasonality. *Environ. Entomol.* 28:924-934.
- [7] Logan, J.A. and J.A. Powell (2001). Ghost Forests, Global Warming and the Mountain Pine Beetle. *American Entomologist* 47: 163.
- [8] Plant, R.E. and L.T. Wilson (1986). Models for age structured populations with distributed maturation rates. *J. Math. Biology.* 23:247-262.
- [9] Powell, J.A., J. Jenkins, J.A. Logan, and B.J. Bentz (2001). Seasonal temperature alone can synchronize life cycles. *Bulletin of Math. Biology.* 62:977-998.
- [10] Reid, R. W. (1962). Biology of the mountain pine beetle, *Dendroctonus monticolae* Hopkins, in the East Kootenay region of British Columbia. I. Life cycle, brood development and flight periods. *Can. Entomol.* 94:531-538.
- [11] Sharpe, P.J.H., G.L. Curry, D.W. DeMichele, and C.L. Cole (1977). Distribution Model of Organism Development Times. *J. Theor. Biol.* 66:21-38.

- [12] Sharpe, P.J.H., and D.W. DeMichele (1977). Reaction Kinetics of Poikilotherm Development. *J. Theor. Biol.* 64:649-670.
- [13] Vansickle, J. (1977). Attrition in Distributed Delay Models. *IEEE Transactions on Systems, Man, and Cybernetics.* 7(9):635-638.
- [14] Von Foerster, H. (1959). *The Kinetics of Cellular Proliferation* (Stohman, F. Jnr. Ed.), pp. 382-407. New York: Grune and Stratton.
- [15] Watson, F.L. (1973). Ph.D. Thesis. University of Arizona, Tucson, Arizona.

## 6 Appendix A

The premise of the Green's function solution is to write each life stage's population density,  $p(1, t)$ , as a function of some previous population density  $f(\tau)$ .

$$p(1, t) = \int_0^t G_a(t, \tau) f(\tau) d\tau$$

The Green's function can be determined from the fundamental solution,  $F$ , which satisfies:

$$\frac{\partial F}{\partial t} + r(T(t)) \frac{\partial F}{\partial a} - \nu \frac{\partial^2 F}{\partial a^2} = 0, \quad F(a, 0) = \delta(a). \quad (17)$$

To obtain a solution to Equation (17) let:

$$z = a - \int_{t_0}^t r(T(\tau)) d\tau, \quad \tau = t.$$

After the change of variables (17) can be written as:

$$\frac{\partial F}{\partial \tau} - \nu \frac{\partial^2 F}{\partial z^2} = 0, \quad F(z, 0) = \delta(z). \quad (18)$$

This is the second order heat equation with solution (19).

$$F(z, \tau) = \frac{1}{\sqrt{4\pi\nu\tau}} \exp\left[-\frac{z^2}{4\nu\tau}\right], \quad 0 < \tau. \quad (19)$$

Inverting the change of variables yields:

$$F_+(a, t) = \frac{H(t - t_0)}{\sqrt{4\pi\nu(t - t_0)}} \exp\left[-\frac{(a - \int_{t_0}^t r(T(s) ds))^2}{4\nu(t - t_0)}\right],$$

and solving this equation when  $r'(T(t)) = -r(T(t))$  the solution is:

$$F_-(a, t) = \frac{H(t - t_0)}{\sqrt{4\pi\nu(t - t_0)}} \exp\left[-\frac{(-a + \int_{t_0}^t r(T(s) ds))^2}{4\nu(t - t_0)}\right].$$

Taking the difference of  $F_+$  and  $F_-$  imparts the property  $G(0, t) = 0$ , and taking the normal derivative with respect to  $a$  gives us the Green's function for the problem:

$$G_a(1, t) = \frac{H(t - t_0)}{\sqrt{4\pi\nu(t - t_0)^3}} \exp\left[-\frac{(1 - \int_{t_0}^t r(T(s) ds))^2}{4\nu(t - t_0)}\right].$$

Therefore the solution for  $p(1, t)$  can be written as,

$$p(1, t) = \int_0^t f(\tau) \frac{H(t - \tau)}{\sqrt{4\pi\nu_1(t - \tau)^3}} \exp\left[-\frac{(1 - \int_{\tau}^t r_1(T(s)) ds)^2}{4\nu_1(t - \tau)}\right] d\tau. \quad (20)$$

## 7 Appendix B

The parameter values are given by:

$$P = \begin{bmatrix} .3148 & 19.95 & .2034 & 29.60 & 4.885 \\ .6887 & 57.28 & .3004 & 25.22 & 4.596 \\ .3562 & 18.01 & .4788 & 19.36 & 3.470 \\ .1909 & 19.70 & .1542 & 8.768 & 7.905 \\ 10.95 & .0100 & nan & nan & nan \\ 11.76 & .0172 & nan & nan & nan \\ 0.095 & 11.85 & -.627 & 30.00 & nan \\ .1690 & .0194 & 1.540 & .8000 & 2.000 \end{bmatrix}$$

where *nan* stands for "not a number", or an empirical parameter that has not been determined. These undetermined values do not affect the performance of the model. The rate functions for the eight life stages were determined empirically in the laboratory. Beetles were incubated in lodgepole pine phloem and the number of days to emergence for each individual was recorded. The developmental rate for the sample is then defined as the inverse of the total days for the median individual. The experiment was performed at several temperatures and the developmental rates were calculated for each. Then curves were fitted to the empirical data to produce developmental rate functions. These empirically determined functions appear below [3].

### Stage 1 (egg)

$$T_1 = T(t) - P(8, 5),$$

where  $T(t)$  is the temperature vector,  $P$  is the parameter matrix, and all values of  $T_1$  that are less than 0 are set to 0.

$$\tau = \frac{T_1}{P(8, 4)}$$

$$r = P(8, 1) \frac{(e^{P(8,2)T_1^{P(8,3)}} - e^{-\tau})(2.54)}{32}$$

### Stages 2,3,and 4 (larval 1, larval 2, and larval 3 )

$$\begin{aligned}
 z1 &= \frac{1}{1 + \mathbf{P}(i-1, 2) * e^{-\mathbf{P}(i-1, 3)T}} \\
 z2 &= e^{-\frac{\mathbf{P}(i-1, 4) - T}{\mathbf{P}(i-1, 5)}} \\
 r &= \mathbf{P}(i-1, 1)(z1 - z2),
 \end{aligned}$$

where  $i$  is the life stage (2,3, or 4). The values of  $r$  less than zero are then set to zero.

#### Stage 5 (larval 4)

$$\begin{aligned}
 xT &= T - \mathbf{P}(4, 5) \\
 \tau &= \frac{(\mathbf{P}(4, 2) - xT)}{\mathbf{P}(4, 3)} \\
 x1 &= \frac{xT^2}{(xT^2 + \mathbf{P}(4, 4)^2)} \\
 x2 &= \mathbf{P}(4, 1)(1 - e^{-\tau}) \\
 r &= x1 + x2 - \mathbf{P}(4, 1),
 \end{aligned}$$

Then the values of  $r$  less than zero, and those with indices  $T < \mathbf{P}(5, 5)$  are set equal to zero.

#### Stages 6 and 7 (pupal and teneral adult)

$$r = \mathbf{P}(i-1, 2)(T - \mathbf{P}(i-1, 1)),$$

where  $i$  is the life stage (6 or 7). Then the values of  $r$  less than zero are set to zero.

#### Stage 8 (ovipositional adult)

All values of  $T$  greater than  $\mathbf{P}(7, 4)$  are set equal to  $2 * \mathbf{P}(7, 4) - T$ . Then:

$$r = \frac{\mathbf{P}(7, 1)}{1 + e^{(\mathbf{P}(7, 2) + \mathbf{P}(7, 3) + T)}}$$

where  $T$  is the temperature vector and  $\mathbf{P}$  is the parameter matrix.